**Supplemental Material**

**Online Table I** –Average read counts of every detected gene in each of the 4 clusters and the variance across subsets from the scRNAseq analysis of *Apoe*$^{-/-}$ mice fed WD for 12 weeks (Fig. 1).

**Online Table II** Enzymatically digested aortas from *Apoe*$^{-/-}$*Cx3cr1*$^{GFP/+}$*Cd11c*$^{YFP}$ mice fed WD for 5 months were analyzed by flow cytometry and live CD45+ cells from were separated into GFP, YFP, DP, and DN groups. Among each group, the frequencies of cells with all combinations of the tested markers (F4/80, CD64, CD11b, CD11c, MHCII) is provided, as average and standard deviation of n=8 mice. No CD11b- CD64+ cells were found. See Fig. 2.

**Online Table III** – Using the transcriptomes of GFP+, DP, YFP+, and DN cells, differential expression was calculated between all pairs of subsets with DESeq2 (6 total comparisons). Only genes that showed a Benjamini-Hochberg adjusted p<.05 and a log-fold change of >2 or <-2 in at least one comparison were considered differentially expressed. If a gene was upregulated in 2 comparisons, it was assigned to the group with the highest expression (or lowest, for downregulated genes). This table lists the 892 individual genes DE genes, divided into 8 lists (up and downregulated for each of the 4 fluorescent groups). Many are statistically upregulated in 1 group and downregulated in another. See Fig. 4a.

**Online Table IV**- "Canonical Pathways" that are enriched (p<.05, calculated in IPA with Right-Tailed Fisher's Exact Test) in the DE gene list. The pathways are organized by enrichment ratio. See Online Table III and Figure 4b.

**Online Table V**- IPA was used to calculate z-scores for the activation or inhibition of "diseases and biological functions" of the GFP, DP, and YFP groups compared to the DN as reference based on the expression of the 892 DE genes. A positive score indicates activation and a negative score indicates inhibition. The functions are organized by the sum of the absolute values of the z-scores. See Online Table I and Fig. 4c.

**Online Table VI**- PRESTO was used to find coexpressed genes in the 18 transcriptomes that passed the QC filters (Online Figure I). Normalized counts were used as an input and filtering for highly variable genes selected 3467 genes. tSNE dimensionality reduction revealed 4 large clusters of genes that share expression patterns across the samples (Fig. 5a). This table lists the genes in each of the clusters.

**Online Table VII**- Each of the gene clusters found using PRESTO analysis was examined with IPA to find the "diseases and biological pathways" that were are enriched in each group. The broad category, specific function, enrichment p-value (Right-Tailed Fisher's Exact Test), and list and number of detected genes in that pathway are shown (Fig. 5b).

**Online Table VIII**- The upregulated genes of each subset (Fig. 4a and Online Table III) were compared to various published transcriptomes using GSEA (Fig. 6a-e). For the comparisons showing significant (FDR<.05) enrichment, the leading genes of the enriched subset are shown. All genes are organized from the most enriched to the least.

**Online Figure I**- Fluorescence-minus-one (FMO) controls for the flow cytometry gates (Fig. 2). Cells from a pool of enzymatically digested aortas from Apoe$^{-/-}$ WD-fed mice were divided into stained or FMO groups for the antibody stains to demonstrate specificity. Single color *Cx3cr1*$^{GFP/+}$ *Apoe*$^{-/-}$ or *Cd11c*$^{YFP}$ *Apoe*$^{-/-}$ mice (both WD fed) were used test the GFP and YFP gates.

**Online Figure II**- Aortas and carotid arteries from 25 *Apoe*$^{-/-}$*Cx3cr1*$^{GFP/+}$*Cd11c*$^{YFP}$ mice fed WD for 5 months (pooled into n=6 samples) were enzymatically digested, gated on live CD45+ cells, and sorted into GFP, DP, YFP, and DN groups using fluorescence activated cell sorting. Sequencing was performed in 2 batches, with samples 1-2 being sequenced together and samples 3-6 sequenced afterwards. A) The number of mice and total collected cells for each sample are shown. B) The 5'->3' coverage graphs were used to filter out low quality samples. Most samples have even coverage, but 6 samples show a distinctive 3' bias. C) In batch 1, 2 samples (2_YFP and 2_DN) were excluded. In batch 2, 4 samples (3_DP, 4_DN, 5_DN, 6_DP) were excluded. 18 samples of the original 24 passed this quality control step. D) The nucleotide frequency graphs showed a similar pattern, with the 6 samples that were excluded showing strong AT bias, and the remaining 18 samples having near even distribution of nucleotides.

**Online Video I-** Example intravital video of a YFP macrophage migrating in the carotid artery of an atherosclerotic *Apoe*$^{-/-}$*Cx3cr1*$^{GFP/+}$*Cd11c*$^{YFP}$ mouse fed WD for 3 months. ILTIS triggering and image processing was used to acquire the data, and custom linear unmixing was used to better separate GFP (green) from YFP (red). DP cells appear yellow. This is a maximum intensity projection of 35 steps through 102 μm of the arterial wall. 15 min movie. Scale bar = 20 μm.

**Online Video II-** Example intravital video of GFP and DP macrophages "dancing-on-the-spot" in the carotid artery of an atherosclerotic *Apoe*$^{-/-}$*Cx3cr1*$^{GFP/+}$*Cd11c*$^{YFP}$ mouse fed WD for 3 months. ILTIS triggering and image processing was used to acquire the data, and custom linear unmixing was used to better separate GFP (green) from YFP (red). DP cells appear yellow. This is a maximum intensity projection of 40 steps through 117 μm of the arterial wall. The round, fast-moving green cells are monocytes in the blood flow. 55 min movie. Scale bar = 50 μm.

## ONLINE METHODS

### Mice

*Apoe*$^{-/-}$ mice were obtained from Jackson Laboratories. *Cd11c*$^{YFP}$ mice were provided by M. Nussenzweig (Rockefeller University, New York).[1] *Cx3cr1*$^{GFP}$ mice were provided by S. Jung (Weizmann Institute of Science, Israel) [2]. Mice were kept in specific pathogen-free conditions in an AAALAC-approved barrier facility, and all experiments were performed in accordance with IACUC standards. Cd11cYFP mice and Cx3cr1GFPmice were both bred onto the *Apoe*$^{-/-}$ background. The independent strains were then bred to each other to create the *Cx3cr1*$^{GFP/+}$ *Cd11c*$^{YFP}$ *Apoe*$^{-/-}$ strain used in this study. The *Cd11c*$^{YFP}$ transgene was screened using the following primers for CD11c and YFP, respectively: 5′-TGC TGG TTG TTG TGC TGT CTC ATC-3′ and 5′-GGG GGT GTT CTG CTG GTA GTG GTC-3′. The Cx3cr1 wild type allele was screened for using the following primers: 5′-TTC ACG TTC GGT CTG GTG GG-3′ and 5′-CGT CTG GAT GAT TCG GAA GTA GC-3′. The GFP knock-in construct was screened with the following primers: 5′-TAA ACG GCC ACA AGT TCA GCG-3′ and 5′-TAC TCC AGC TTG TGC CCC AGG ATG TT-3′. RT-PCR testing was conducted by Transnetyx. All mice were fed WD starting at 6 to 8 weeks of age.

### Flow Cytometry and Fluorescence-Activated Cell Sorting

For cell surface marker analysis, aortas were taken from male and female *Cx3cr1*$^{GFP/+}$ *Cd11c*$^{YFP}$ *Apoe*$^{-/-}$ mice that had been fed WD for 5 months. The tissue was enzymatically digested[3] for 45 minutes using a 450 U/ml collagenase type I, 250 U/ml collagenase type XI, 120 U/ml hyaluronidase, and 12.5 Kunitz/mL DNAase in HBSS. Tissue remaining after the first digestion was given fresh enzymatic buffer and allowed to continue to digest for an additional 30-60 min, while freed cells were collected. After washing, the cells were stained for CD45-APC-Cy7 (clone 30-F11), CD64-APC (clone X54-5/7.1), CD11b-BV510 (clone M1/70), CD103-BV421 (clone 2E7), CD11c-PE-Cy7 (clone N418), F4/80-PE (clone CI:A3-1), MHCII-AF700 (clone M5/114.15.2), and 7AAD. Single cells were analyzed with a BD LSRII. Gates were determined by fluorescence-minus-one controls. All analysis was performed in FlowJo (Tree Star).

For sorting arterial leukocytes for RNA sequencing, aortas and carotid arteries were taken from male and female *Cx3cr1*$^{GFP/+}$ *Cd11c*$^{YFP}$ *Apoe*$^{-/-}$ mice that had been fed WD for 5 months. The same digestion protocol as above was used, except all arteries from 3-4 mice were pooled. RNase out was put into the digestion buffer. Cells were stained with a smaller panel F4/80, CD11b, CD11c, CD45, and 7AAD. After gating for live CD45+ singlet cells, cells were sorted into GFP, DP, YFP, and DN populations into Trizol LS using a FACSAria II. The F4/80, CD11b, and CD11c were used to confirm the expected cell proportions were obtained.

### RNA sequencing and analysis

RNA was extracted from the sorted GFP, DP, YFP, and DN cells using an RNeasy Mini Kit (Qiagen). At this stage, two sets of samples were combined because too few cells had been sorted. Total RNA was processed using SMART-seq v4 Ultra Low Input RNA Kit (Clonetech) following manufacturer's instructions. cDNA was amplified using 11 cycles and eluted in 12 μL. 5 μL of resulting cDNA was processed using a NexteraXT kit (Illumina) following manufacturer's instructions. Samples were pooled into two batches and sequenced with Single Read 50 base pair (SR50) reads on an Illumina HiSeq4000.

Reads that passed Illumina filters were filtered for reads aligning to tRNA, rRNA, adapter sequences, and spike-in controls. The reads were then aligned to the mm10 reference genome and NCBI annotations using TopHat (v 1.4.1)[4]. DUST scores were calculated with PRINSEQ Lite (v 0.20.3)[5] and low-complexity reads (DUST > 4) were removed from the BAM files. The alignment results were parsed via the SAMtools[6] to generate SAM files. Read counts to each genomic feature were obtained with the htseq-count program (v 0.7.1)[7] using the "union" option.

Post-mapping quality control checks were used to exclude poor quality samples using RSeqC v2.6[8]. 6 out of 24 samples were removed due to having uneven gene body coverage. These 6 samples also showed higher AT content and more reads mapped outside of exons. The remaining 18 samples were used for all subsequent analysis.

Only genes with a raw read count >7 in at least one sample were used. Differential expression was calculated between all pairs of samples (6 total tests) using DESeq2[9]. Genes were filtered for those that had a Benjamini-Hochberg adjusted $p<0.05$ and a log fold change $\geq 2$ in at least one comparison. 892 genes passed these criteria and were called differentially expressed. Genes that were differentially upregulated by more than one group based on these criteria were assigned to the group with the highest expression based on log fold change (or the reverse, for downregulated genes). Morpheus (Broad Institute) was used to generate all heat maps and hierarchical clustering. GSEA[10] was performed with GenePattern[11] (Broad Institute), using standard settings, except with a minimum set size of 10 and gene-based permutations. Enriched and activated pathways were calculated in Ingenuity Pathway Analysis (Qiagen)[12] using default settings.

**Single Cell RNA sequencing**

Raw data for the single cell RNAseq was taken from previously work, and the methods have been described[13]. Aortas from 10 *Apoe*$^{-/-}$ mice fed WD for 12 weeks were enzymatically digested and pooled. Live CD45+ leukocytes were sorted and loaded on the Chromium Single Cell Controller (10xGenomics) to obtain individual gel bead emulsions containing single cells. 2077 live aortic leukocytes from the pooled, sorted cells were successfully encapsulated. Single cell RNA libraries were prepared using the Single Cell 3' Solution v2 Reagent Kit (10xGenomics). The obtained libraries were quantified post construction by quantitative PCR (Kapa DNA Quantification Kit for Illumina platforms). Subsequently, the quantified and constructed libraries were sequenced on HiSeq2500 with a rapid run. For this, a HiSeq Rapid Cluster Kit V2 – Paired End and a HiSeq Rapid SBS Kit V2 were used. Single cell transcriptomes were processed using the Cell Ranger Single Cell software suite version 1.3. and mapped to the mouse reference transcriptome mm10 applying STAR.

Cells expressing both *Adgre* and *Cd68* were selected with the SeqGeq genomic gating tool (Treestar Software) and filtered for the top 250 genes with the highest variance across all cells within this data set. This gene set was used as input for t-SNE with a perplexity of 7, with calculations performed in Matlab[14]. K-means clustering on the 2D t-SNE plot was performed in Matlab using an adapted algorithm that automatically determines the number of clusters based on a standard significance levels[15]. Based on a significance of 0.2, 4 major populations were retrieved. Differentially expressed genes were next filtered with the Comparative Marker Suite (GenePattern, Broad Institute) with cutoffs for FDR<5% (Benjamini Hochberg) and $p<0.05$ (two-sided T-test, 10000 permutations) on the full gene set of all macrophages in

the 4 populations (one-versus-all comparison). Genes were displayed in column minimum-maximum value heatmaps by Morpheus (GenePattern, Broad Institute) followed by free hierarchical clustering (one-minus-pearson with average linkage). Pathway activation was calculated in Ingenuity Pathway Analysis applying the core analysis feature (Qiagen)[51].

**Imaging**

Aortas and carotid arteries from *Cx3cr1*$^{GFP/+}$ *Cd11c*$^{YFP}$ *Apoe*$^{-/-}$ mice fed WD were used for all imaging experiments. For whole mount imaging, aortas were fixed with 4% paraformaldehyde and stained with Hoechst. The tissue was imaged with a Leica SP5 multiphoton microscope with a Ti-Sapphire laser (Chameleon Ultra II, Coherent), tuned to 920 nm, and a resonant scanhead for fast scanning, and a water-dipping objective (Olympus XLUMPLFL 20X NA 0.95). The emitted light was split into three photomultiplier tube detectors by two dichroic mirrors (520 and 495 nm) and three filters (513/17 nm for GFP, 513/22 nm for YFP, and 460/50 nm for Hoescht).

ILTIS[16] intravital imaging utilized the same optical set-up, though the blue channel was used to detect collagen via second harmonic generation instead of Hoescht. Mice were anesthetized with a mixture of ketamine/xylazine/atropine (100/10/0.4mg/kg intraperitoneally). A tracheal cannula was placed to help the mice breathe and the mice were given supplemental oxygen near the cannula. Supplemental intravenous anesthetic was given through a jugular cannula as necessary. The right carotid artery was gently surgically exposed and kept wet with heated phenol-free RPMI. A pulse-oximeter was used monitor the heartbeat and to trigger image acquisition during approximate diastole. 3 single images in 3 heartbeats were taken at each location at each timepoint, and stacks of 25-40 z steps (3-5 μm apart) were acquired every 30-50 seconds.

Ex vivo imaging was performed similarly to previous work[17], but was performed on a Leica SP8 with HyD GaAsP detectors. The explanted aorta was kept in a dish with heated, oxygenated, circulating RPMI during imaging. The same excitation wavelength and emission filters were used as above.

**Image Processing**

Image sequences from the intravital experiments were converted to 3D movies as described previously[16]. Briefly, one out of each set of 3 images taken sequentially at a single location was selected based on a global optimization algorithm. Then, after being converted to a 4-dimensional hyperstack, Mistica minimum spanning tree-based course image alignment[18] registered the images to create the final 3-dimensional movies.

For the qualitative evaluation of cell motion, maximum intensity projections of the intravital movies were generated and the GFP and YFP channels were assigned random pseudocolors. The movies were given to blinded judge unfamiliar with the work who was asked to judge each macrophage as “dancing”, “migrating”, or not moving. Monocytes (small, round cells, moving in a single direction due to blood flow) were skipped. Only healthy cells showing some discernible movement were used for the statistics.

Segmentation of macrophages in tissue is a notoriously difficult problem. In these mice, elongated cells with varying ratios of GFP and YFP were often located next to each other. To more accurately segment these cells in the intravital movies, we adapted dynamic color gradient thresholding[19] to create a novel 3D

segmentation algorithm. Instead of relying purely on intensity thresholds, this identifies cell boundaries based on gradients and covariances of the intensities of GFP and YFP. The cells are first loosely segmented in Imaris, and then all cellular pixel data is transferred to Matlab. Smooth regions of minimal change in intensity, and then iteratively grown towards the cell boundaries. We altered the original algorithm to process 3D images and to ensure that no cell is ever fully enclosed by another. Surfaces were generated in Matlab and then transferred to Imaris, where they were manually altered as necessary. Tracking over time was performed semi-automatically in Imaris, and then the edited tracks were transferred back to Matlab for further quantification.
"Centroid-adjusted Dancing" is a measure of how much a cell's shape changes between two timepoints. The 3D outline of each cell was shifted so that it's center point was colocalized with the centroid of that cell in the previous time point. "Dancing" is the total number of voxels occupied by only 1 of the two cells divided by the total number of voxels in either cell, normalized to the time step. In other words, the dancing index is calculated as:

$$DI = \frac{\sum V_1 + \sum V_2}{\sum V_{1+2}} \Big/ t_2 - t_1$$

where $V_x$ represents the voxels present only in frame X, $V_{x+y}$ are the voxels occupied in either timepoints x and y, and $t_x$ is the time when frame X was acquired.

The images of aorta explants acquired on the SP8 were processed using a pixel classification tool (iLastik[20]), trained to recognize cells or background. The probability maps and raw channel intensities were imported into Matlab to calculate shape statistics.

All images were processed with a custom written linear unmixing script to reduce bleed through between the GFP and YFP channels. This script imports the mean intensity in the GFP and YFP channels of cells defined in Imaris (Bitplane) into Matlab. These cell intensities are displayed as a scatter plot, and the user may manually adjust a bleedthrough weighting table until the cells are maximally separated, similar to widely-used compensation in FlowJo (Tree Star). Matlab performs pixel-by-pixel linear unmixing using the determined weighting factors and exports corrected images for the 2 channels.

All image processing statistics were calculated in Prism.

**References for Online Materials**


1. Lindquist RL, Shakhar G, Dudziak D, Wardemann H, Eisenreich T, Dustin ML, Nussenzweig MC. Visualizing dendritic cell networks in vivo. *Nature Immunology*. 2004;5:1243–1250.
2. Jung S, Aliberti J, Graemmel P, Sunshine MJ, Kreutzberg GW, Sher A, Littman DR. Analysis of Fractalkine Receptor CX3CR1 Function by Targeted Deletion and Green Fluorescent Protein Reporter Gene Insertion. *Molecular and Cellular Biology*. 2000;20:4106–4114.
3. Butcher MJ, Herre M, Ley K, Galkina E. Flow Cytometry Analysis of Immune Cells Within Murine Aortas. *Journal of Visualized Experiments : JoVE*. 2011.
4. Trapnell C, Pachter L, Salzberg SL. TopHat: discovering splice junctions with RNA-Seq. *Bioinformatics (Oxford, England)*. 2009;25:1105–1111.
5. Schmieder R, Edwards R. Quality control and preprocessing of metagenomic datasets. *Bioinformatics (Oxford, England)*. 2011;27:863–864.
6. Li H, Handsaker B, Wysoker A, Fennell T, Ruan J, Homer N, Marth G, Abecasis G, Durbin R, 1000 Genome Project Data Processing Subgroup. The Sequence Alignment/Map format and SAMtools. *Bioinformatics (Oxford, England)*. 2009;25:2078–2079.
7. Anders S, Pyl PT, Huber W. HTSeq--a Python framework to work with high-throughput sequencing data. *Bioinformatics (Oxford, England)*. 2015;31:166–169.
8. Wang L, Wang S, Li W. RSeQC: quality control of RNA-seq experiments. *Bioinformatics (Oxford, England)*. 2012;28:2184–2185.
9. Love MI, Huber W, Anders S. Moderated estimation of fold change and dispersion for RNA-seq data with DESeq2. *Genome Biology*. 2014;15:550.
10. Subramanian A, Tamayo P, Mootha VK, Mukherjee S, Ebert BL, Gillette MA, Paulovich A, Pomeroy SL, Golub TR, Lander ES, Mesirov JP. Gene set enrichment analysis: A knowledge-based approach for interpreting genome-wide expression profiles. *Proceedings of the National Academy of Sciences*. 2005;102:15545–15550.
11. Reich M, Liefeld T, Gould J, Lerner J, Tamayo P, Mesirov JP. GenePattern 2.0. *Nature Genetics*. 2006;38:500–501.
12. Krämer A, Green J, Pollard J, Tugendreich S. Causal analysis approaches in Ingenuity Pathway Analysis. *Bioinformatics (Oxford, England)*. 2014;30:523–530.
13. Winkels H, Ehinger E, Vassallo M, Buscher K, Dinh H, Kobiyama K, Hamers A, Cochain C, Vafadarnejad E, Saliba A-E, Zernecke A, Pramod A, Ghosh A, Michel NA, Hoppe N, et al. Atlas of the Immune Cell Repertoire in Mouse Atherosclerosis Defined by Single-Cell RNA-Sequencing and Mass Cytometry. *Circulation Research*. 2018:CIRCRESAHA.117.312513.
14. Maaten L van der, Hinton G. Visualizing Data using t-SNE. *Journal of Machine Learning Research*. 2008;9:2579–2605.
15. Hamerly G, Elkan C. Learning the k in k-means. *Advances in neural information processing systems*. 2004:8.
16. McArdle S, Chodaczek G, Ray N, Ley K. Intravital live cell triggered imaging system reveals monocyte patrolling and macrophage migration in atherosclerotic arteries. *Journal of Biomedical Optics*. 2015;20:26005.
17. Koltsova EK, Garcia Z, Chodaczek G, Landau M, McArdle S, Scott SR, von Vietinghoff S, Galkina E, Miller YI, Acton ST, Ley K. Dynamic T cell-APC interactions sustain chronic inflammation in atherosclerosis. *The Journal of Clinical Investigation*. 2012;122:3114–3126.
18. Ray N, McArdle S, Ley K, Acton ST. MISTICA: Minimum Spanning Tree-Based Coarse Image Alignment for Microscopy Image Sequences. *IEEE journal of biomedical and health informatics*. 2016;20:1575–1584.
19. Balasubramanian GP, Saber E, Misic V, Peskin E, Shaw M. Unsupervised color image segmentation using a dynamic color gradient thresholding algorithm. In: *Human Vision and Electronic Imaging XIII*.Vol 6806. International Society for Optics and Photonics; 2008:68061H.

20. Sommer C, Straehle C, Kothe U, Hamprecht FA. Ilastik: Interactive learning and segmentation toolkit. In: *2011 IEEE International Symposium on Biomedical Imaging: From Nano to Macro*. Chicago, IL, USA: IEEE; 2011:230–233.

A

| Sample Number | GFP | | | | | | DP | | | | | | YFP | | | | | | DN | | | | | |
|---|---|---|---|---|---|---|---|---|---|---|---|---|---|---|---|---|---|---|---|---|---|---|---|---|
| | 1 | 2 | 3 | 4 | 5 | 6 | 1 | 2 | 3 | 4 | 5 | 6 | 1 | 2 | 3 | 4 | 5 | 6 | 1 | 2 | 3 | 4 | 5 | 6 |
| Pooled Mice | 7 | 4 | 3 | 3 | 4 | 4 | 7 | 4 | 3 | 3 | 4 | 4 | 7 | 4 | 3 | 3 | 4 | 4 | 7 | 4 | 3 | 3 | 4 | 4 |
| Cell Number | 1245 | 3811 | 5439 | 3737 | 4251 | 5926 | 2548 | 5074 | 11303 | 12719 | 4724 | 7616 | 318 | 626 | 892 | 2037 | 451 | 566 | 2066 | 2881 | 1075 | 694 | 676 | 641 |

B

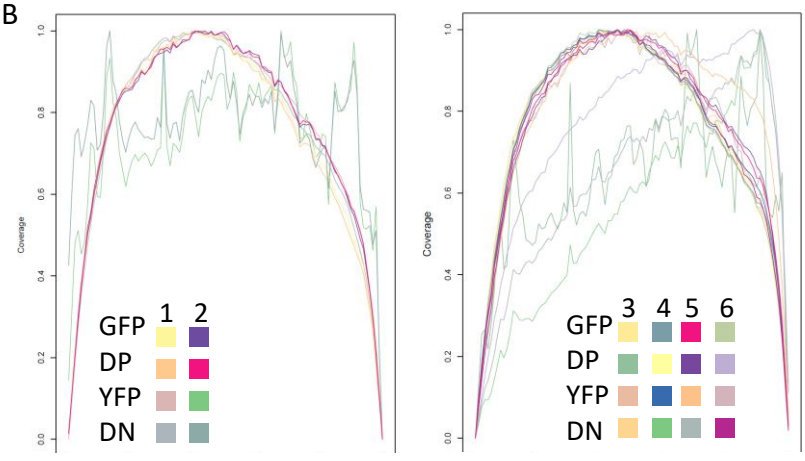


Gene Body Percentile 5'->3'  Gene Body Percentile 5'->3'

C

| Passed QC? | | | | | | | |
|---|---|---|---|---|---|---|---|
| | 1 | 2 | 3 | 4 | 5 | 6 | **Total n** |
| GFP | x | x | x | x | x | x | 6 |
| DP | x | x | | x | x | | 4 |
| YFP | x | | x | x | x | x | 5 |
| DN | x | | x | | | x | 3 |

D

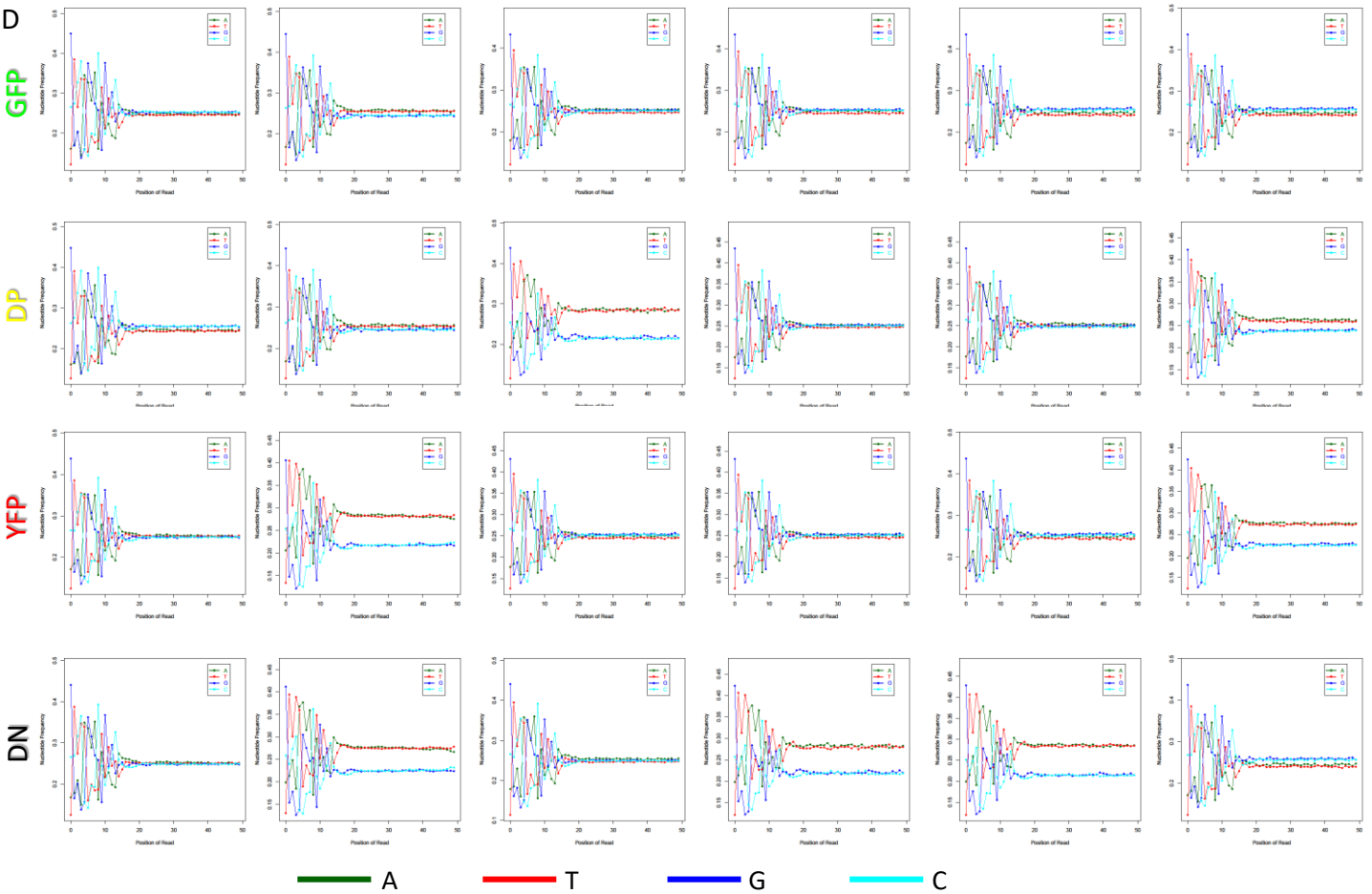


Online Figure I

A

| Sample | GFP | | | | | | DP | | | | | | YFP | | | | | | DN | | | | | |
|---|---|---|---|---|---|---|---|---|---|---|---|---|---|---|---|---|---|---|---|---|---|---|---|---|
| Number | 1 | 2 | 3 | 4 | 5 | 6 | 1 | 2 | 3 | 4 | 5 | 6 | 1 | 2 | 3 | 4 | 5 | 6 | 1 | 2 | 3 | 4 | 5 | 6 |
| Pooled Mice | 7 | 4 | 3 | 3 | 4 | 4 | 7 | 4 | 3 | 3 | 4 | 4 | 7 | 4 | 3 | 3 | 4 | 4 | 7 | 4 | 3 | 3 | 4 | 4 |
| Cell Number | 1245 | 3811 | 5439 | 3737 | 4251 | 5926 | 2548 | 5074 | 11303 | 12719 | 4724 | 7616 | 318 | 626 | 892 | 2037 | 451 | 566 | 2066 | 2881 | 1075 | 694 | 676 | 641 |

B

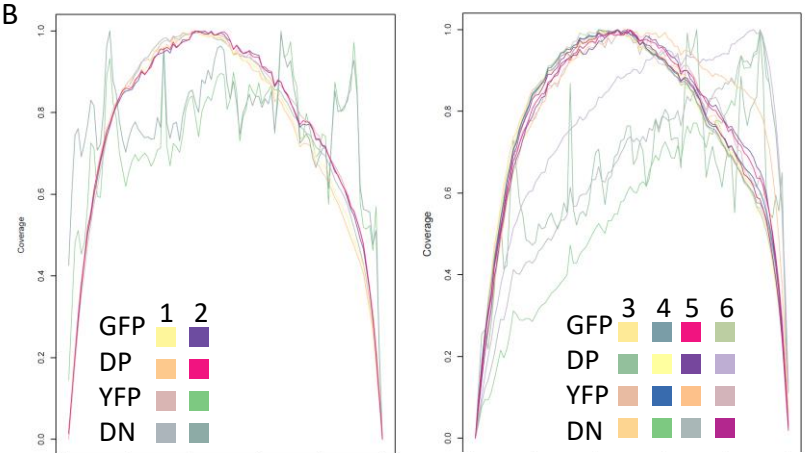


Gene Body Percentile 5'->3'  Gene Body Percentile 5'->3'

C

| Passed QC? | | | | | | | |
|---|---|---|---|---|---|---|---|
| | 1 | 2 | 3 | 4 | 5 | 6 | **Total n** |
| GFP | x | x | x | x | x | x | 6 |
| DP | x | x | | x | x | | 4 |
| YFP | x | | x | x | x | x | 5 |
| DN | x | | x | | | x | 3 |

D

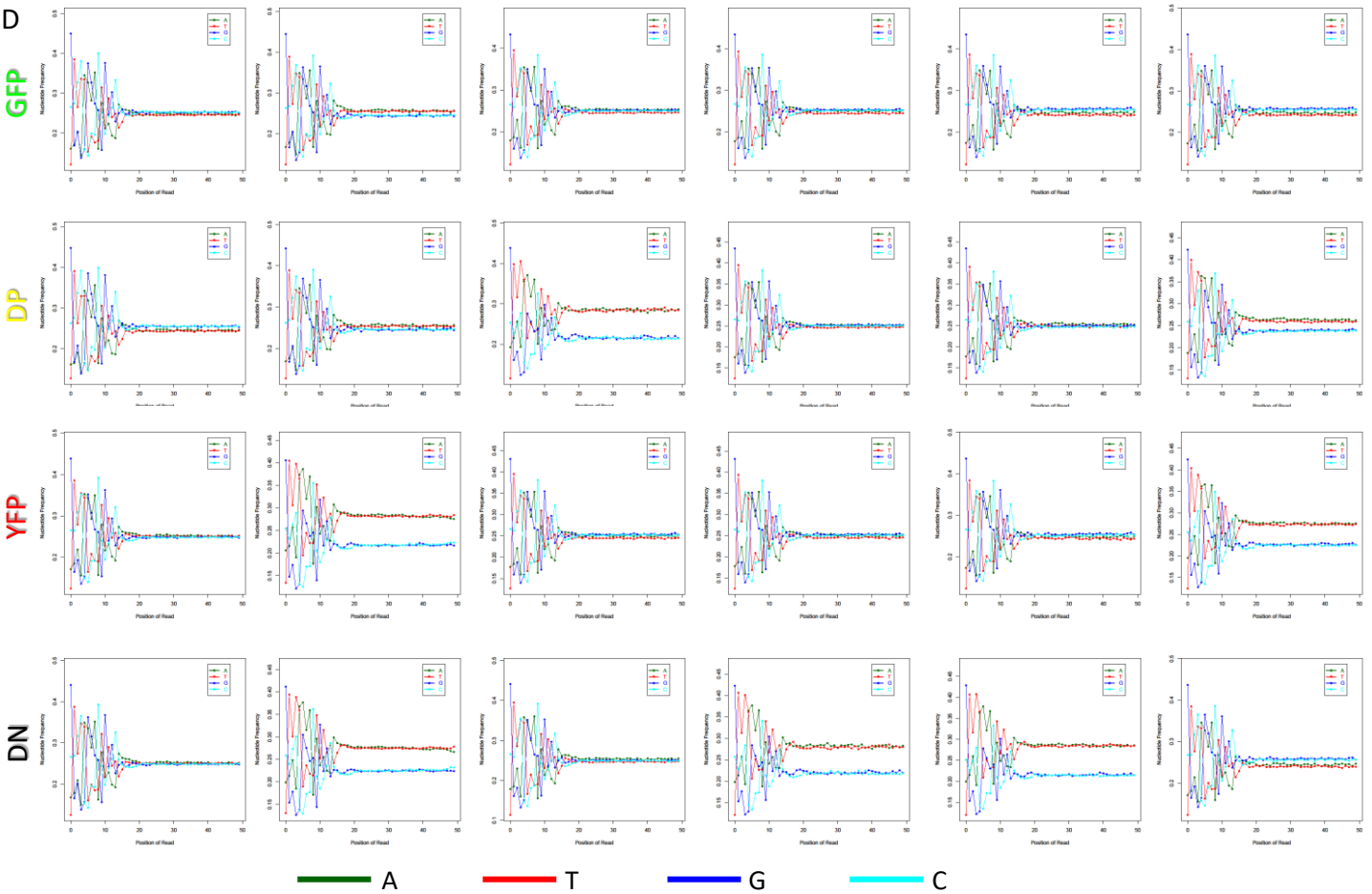


Online Figure II

| | | | | | GFP | | DP | | YFP | | DN | |
|---|---|---|---|---|---|---|---|---|---|---|---|---|
| F4/80 | CD64 | CD11b | CD11c | MHCII | Average | SEM | Average | SEM | Average | SEM | Average | SEM |
| + | + | + | + | + | 4.8 | 0.89 | 19.4 | 2.26 | 15.3 | 4.59 | 0.1 | 0.05 |
| + | + | + | + | - | 8.0 | 1.58 | 19.5 | 2.01 | 13.6 | 2.41 | 0.4 | 0.11 |
| + | + | + | - | + | 22.2 | 2.39 | 17.7 | 4.37 | 10.5 | 2.22 | 0.6 | 0.14 |
| + | + | + | - | - | 22.9 | 3.78 | 8.4 | 1.81 | 13.9 | 4.96 | 4.7 | 1.04 |
| + | - | + | + | + | 1.1 | 0.23 | 3.6 | 0.60 | 1.7 | 0.26 | 0.0 | 0.01 |
| + | - | + | + | - | 6.4 | 1.82 | 11.6 | 3.18 | 4.0 | 1.15 | 0.3 | 0.08 |
| + | - | + | - | + | 2.5 | 0.85 | 2.0 | 0.83 | 1.0 | 0.33 | 0.1 | 0.06 |
| + | - | + | - | - | 9.5 | 1.84 | 5.7 | 1.69 | 2.8 | 0.93 | 9.4 | 2.48 |
| + | - | - | + | + | 0.5 | 0.25 | 0.9 | 0.37 | 3.6 | 1.09 | 0.0 | 0.02 |
| + | - | - | + | - | 0.6 | 0.25 | 0.5 | 0.21 | 1.4 | 0.43 | 0.2 | 0.09 |
| + | - | - | - | + | 0.5 | 0.21 | 0.3 | 0.13 | 10.5 | 5.62 | 4.6 | 1.24 |
| + | - | - | - | - | 8.4 | 1.66 | 0.7 | 0.14 | 6.5 | 0.90 | 46.6 | 2.05 |
| - | + | + | + | + | 0.4 | 0.14 | 1.4 | 0.30 | 0.9 | 0.30 | 0.1 | 0.04 |
| - | + | + | + | - | 0.3 | 0.11 | 0.4 | 0.16 | 0.9 | 0.38 | 0.0 | 0.02 |
| - | + | + | - | + | 0.8 | 0.24 | 0.5 | 0.14 | 0.3 | 0.11 | 0.0 | 0.03 |
| - | + | + | - | - | 1.2 | 0.27 | 0.3 | 0.05 | 0.4 | 0.14 | 1.3 | 0.43 |
| - | - | + | + | + | 0.8 | 0.34 | 1.5 | 0.47 | 0.4 | 0.20 | 0.0 | 0.01 |
| - | - | + | + | - | 0.5 | 0.16 | 0.8 | 0.22 | 1.1 | 0.29 | 0.2 | 0.05 |
| - | - | + | - | + | 0.6 | 0.13 | 0.4 | 0.09 | 0.2 | 0.09 | 0.0 | 0.01 |
| - | - | + | - | - | 1.8 | 0.44 | 0.5 | 0.10 | 0.7 | 0.26 | 5.3 | 1.31 |
| - | - | - | + | + | 0.4 | 0.18 | 0.3 | 0.13 | 0.7 | 0.19 | 0.0 | 0.02 |
| - | - | - | + | - | 0.3 | 0.13 | 0.1 | 0.05 | 0.6 | 0.11 | 0.1 | 0.05 |
| - | - | - | - | + | 0.2 | 0.08 | 0.1 | 0.04 | 2.3 | 1.24 | 2.1 | 0.52 |
| - | - | - | - | - | 4.0 | 1.08 | 0.2 | 0.06 | 2.4 | 0.39 | 23.2 | 2.10 |
| Among all CD45+ | | | | | **27.3** | 2.49 | **36.8** | 2.54 | **10.7** | 1.29 | **25.1** | 2.13 |

Online Table II